AJNR

Structural Changes of the Substantia Nigra in Parkinson's Disease as Revealed by MR Imaging

Michael Hutchinson and Ulrich Raff

AJNR Am J Neuroradiol 2000, 21 (4) 697-701
http://www.ajnr.org/content/21/4/697

AJNR Am J Neuroradiol 21:697–701, April 2000

Structural Changes of the Substantia Nigra in Parkinson's Disease as Revealed by MR Imaging

Michael Hutchinson and Ulrich Raff

BACKGROUND AND PURPOSE: **The possibility of using MR imaging as a sensitive marker of the structural changes in Parkinson's disease has been a long-sought goal. We describe a new method for imaging and quantifying the morphologic changes of the substantia nigra in Parkinson's disease and compare radiologic findings with clinical evaluation.**

METHODS: **Using a combination of two MR imaging inversion-recovery pulse sequences, the substantia nigra was imaged in six patients with Parkinson's disease and six age-related control participants. A radiologic index was defined and used to quantify the signal changes that were observed in the patients. The radiologic index was compared with clinical scores obtained from the Unified Parkinson's Disease Rating Scale.**

RESULTS: **The images showed loss of signal in a lateral-to-medial gradient in cases of Parkinson's disease, corresponding to the known neuropathologic pattern of degeneration. The radiologic index was highly correlated with the Unified Parkinson's Disease Rating Scale score, and there was no overlap in radiologic indices between the patient and the control groups ($P < .00005$).**

CONCLUSION: **This study suggests that MR imaging is sensitive to structural changes in even the earliest cases of Parkinson's disease, thereby indicating the potential for detecting presymptomatic disease. Furthermore, a radiologic measure has been defined that correlates with the conventional clinical measure of disease severity. Therefore, MR imaging could prove to be a sensitive biological marker for objective staging of the disease.**

Parkinson's disease is a common, progressive neurodegenerative condition involving mainly the degeneration of neurons in the substantia nigra pars compacta (SN_C). Approximately 10% to 20% of all cases may be familial and inherited in an autosomal dominant pattern with incomplete penetrance (1). There is general consensus that at the onset of symptoms, the majority of neurons in the SN_C have degenerated. Although surgical and medical interventions can alleviate the symptoms for many years, they probably do not alter the rate of degeneration. Nevertheless, putative neuroprotective interventions aimed at slowing or even halting disease progression are currently under investigation (2, 3). Therefore, considering the enormous human and socioeconomic costs of Parkinson's disease, the earliest detection, and even the detection of presymptomatic disease, is highly desirable. Furthermore, an objective radiologic measure would be of value for assessing the effects of such interventions in both asymptomatic and symptomatic patients.

Clinical staging is the present standard of reference for following disease progression. The most comprehensive and widely used scale is the Unified Parkinson's Disease Rating Scale (4). Despite its strengths, however, the scale has a number of distinct limitations. Patients have symptoms that fluctuate from day to day, and there may be considerable interobserver variability. These sources of error alone require that clinical trials of drug efficacy must include a large number of participants. Also, by definition, the scale renders one incapable of detecting presymptomatic disease.

At the present time, the most sensitive imaging techniques for the detection of Parkinson's disease are positron emission tomography (5–8) and single-photon emission CT (9–11). Both techniques measure striatal changes, but not changes in the SN_C itself. Positron emission tomography traditionally measures the uptake of dopa in the striatum, whereas single-photon emission CT uses a tracer, β-CIT, which is a label for dopamine transporters. Both techniques are sensitive to disease stage in symptomatic patients and hold the promise for revealing presymptomatic disease. They are, however, rela-

Received June 10, 1999; accepted November 11.

From the Departments of Neurology (M.H., U.R.) and Radiology (M.H.), New York University School of Medicine, New York, NY.

Address reprint requests to Michael Hutchinson, MD, PhD, Department of Neurology, New York University School of Medicine, 550 First Avenue, New York NY 10016.

tively costly and not widely available. Moreover, both techniques require that a patient be off medication for at least 12 hours before the study. This can be uncomfortable for a patient with advanced symptoms, and is potentially dangerous.

On the other hand, MR imaging is a simple and relatively inexpensive technique that is widely available. Its use in this context has therefore been a highly desirable but elusive goal. Various efforts have been made to show nigral changes by using MR imaging. These fall essentially into two categories. The first category is based on the changes in T2 and T2* signal associated with the increased iron deposition in the SN_C occurring in cases of Parkinson's disease (12–14). Iron is deposited in the SN_C in normal aging, however, and this may create difficulties in separating patients from control participants. In particular, in a large study, changes in T2-weighted imaging findings did not correlate either with disease duration or with clinical severity (14). The second category involves measurement of the width of the SN_C (15–17) by using T2-weighted images. Although thinning of this structure does occur in cases of Parkinson's disease, the nucleus is only a few millimeters wide and takes on an irregular appearance as the disease progresses. This makes the width difficult to define with precision.

We have recently developed a different MR imaging approach for evaluating the SN_C, which uses a combination of two pulse sequences, each of the inversion-recovery types, which are therefore heavily T1-weighted. This approach was based on the hypothesis that T1-weighted imaging depends mainly on the intracellular space and that such sequences ought to be sensitive to the changes in intracellular volume occurring with cell death.

One sequence was specifically designed to suppress peduncular white matter and the other to suppress nigral gray matter. These image types are white matter–suppressed (WMS) and gray matter–suppressed (GMS). A combination of these pulse sequences showed structural changes in the substantia nigra in even the earliest cases of symptomatic disease.

Methods

Patients

Six patients in various stages of the disease (Unified Parkinson's Disease Rating Scale scores, 12−71; age range, 38−70 years; mean age, 58 years) and six age-matched, healthy control participants (age range, 37−72 years; mean age, 56 years) underwent imaging. Informed consent was obtained from patients before imaging was performed. All patients were taking their usual anti-Parkinson's disease medication at the time of the imaging. None of the control participants had any known relatives with Parkinson's disease, and all were examined and questioned by an experienced neurologist to rule out signs and symptoms suggestive of early Parkinson's disease.

MR Imaging

Imaging was performed using a Siemens 1.5-T Vision system. To avoid head motion artifacts due to respiration, all patients and participants were immobilized in flexion-extension of the neck by means of a chin strap.

Imaging of the SN_C was performed using two distinct inversion-recovery sequences. The first of these was designed to suppress nigral gray matter, whereas the second was designed to suppress the white matter of the crus cerebri. As previously hypothesized, for patients, the GMS images showed large variations in signal intensity within the SN_C. These signal changes were particularly pronounced at the anterior and lateral edges, making the boundaries of this structure difficult to define in patients with advanced disease. On the other hand, signal variation in the WMS images was less than but in a direction opposite that of the GMS images. In WMS images, the edges of the SN_C were distinct, even in patients with advanced disease. Therefore, by taking the ratio of the two images (WMS/GMS), not only is contrast improved (because the signal changes are additive) but the borders of the SN_C are defined, even in advanced cases. For each pixel in the ratio image, a signal intensity ratio is defined as its value in the WMS image divided by its value in the GMS image.

WMS images were obtained with an inversion-recovery (modulus) pulse sequence of 1450/20 (TR/TE) with an inversion time of 250 ms. GMS images were obtained with a similar inversion-recovery sequence but with parameters of 2000/20 and an inversion time of 420 ms. The field of view was 200 mm, and the image matrix was 256 × 256. The number of acquisitions was two. The section thickness was 3 mm with a gap of 0.2 mm. Four axial sections were obtained in each case, with sections selected from a sagittal scout image of the brain stem. Sections were chosen to be perpendicular to the longitudinal axis of the mesencephalon. The lowest section was taken just at the level of the most rostral part of the pons. Using the WMS image, it was ascertained that the SN_C was visible in each of the four sections. By selecting the middle two sections for analysis, we ensured that there was no contamination by volume averaging.

Data Analysis

The WMS and GMS axial images were used to extract the mesencephalic peduncular structures. Figure 1 shows the original WMS and GMS images obtained through the midbrain in a control participant. A manual region-of-interest technique applied to the WMS images was used to extract simultaneously the cerebral peduncle in WMS and GMS images from adjacent structures (Fig 1, *second row*). Note the improved contrast in the cerebral peduncle is because signal intensities in the WMS image are redisplayed in 256 gray levels whereas, on the contrary, the corticospinal tracts correspond to high intensities in the GMS image. The ratio image (WMS/GMS) of the cerebral peduncle was then computed and displayed in color by using a 256-pseudocolor lookup table.

To obtain a numerical value for the degree of signal change in the SN_C, we took advantage of the known geometric variation in the degeneration of this nucleus (ie, from lateral to medial) (18). All analyses were conducted on the middle two sections of the ratio images by an observer blinded to whether the image was of a patient or a control participant. All images were identified to this observer only as a number. Regions of interest (approximately 200 pixels each) were placed on the lateral and medial segments of the SN_C. For each patient and participant in the study, this ratio was computed for both right and left sides of each of the two sections and the lateral and medial sections of the SN_C. The mean pixel value within each region of interest was then used to define the ratio of pixel values in all four values averaged together to give R_{AV}. As expected, the R_{av} of control participants all had values close

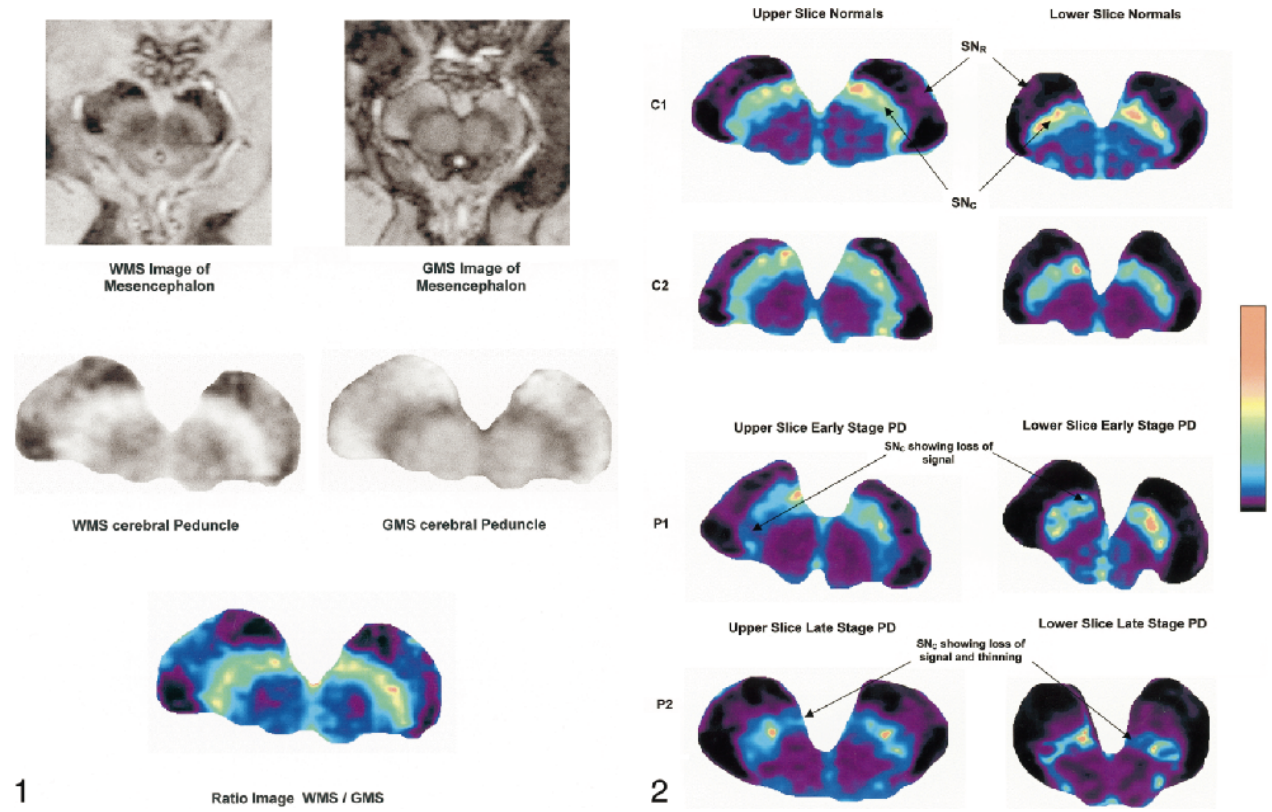

FIG 1. *Upper row* displays an example of axial WMS and GMS MR acquisition images of the mesencephalon in a control participant. The cerebral peduncle (*second row, left*) extracted from the WMS midbrain image serves as a template to extract the GMS image of the cerebral peduncle shown on the *right.* The SN_C is seen as a bright arch in the peduncular WMS image, whereas it appears as a dark band in the corresponding GMS image. Note also the substantia nigra pars reticulata (SN_R) reaching across the crus cerebri toward the SN_C. The ratio image (WMS/GMS) of the two images in the *second row* yields the color-coded ratio image displayed on the *bottom.* All black and white images are shown using a standard display of 256 gray levels. The color image uses a 256-pseudocolor lookup table.

FIG 2. Ratio images of the cerebral peduncle displayed in pseudocolors show the morphologic characteristics of the SN_C in two control participants (C1 and C2) and the structural changes in two patients with Parkinson's disease (P1 and P2). The substantia nigra pars reticulata (SN_R) is indicated for participant C1. Notice that the SN_C in control participants reaches out toward the peduncular edge in the upper section, taking on the form of an arch. In the images of patient P1, who has Parkinson's disease, thinning and loss of signal can be seen in the lateral segment of the SN_C in the upper section. The lower section shows islands of cell loss on both sides of the SN_C. Note the considerable thinning and loss of signal in both upper and lower sections of the images of patient P2, who has late-stage Parkinson's disease. *Left* and *right sides* show two rims of preserved signal.

to one, whereas the patients had a wide range of values. A radiologic index was then defined as follows:

$$RI = 100\ (1 - R_{AV})$$

Results

Because the eye is more sensitive to color than to gray scale, rendering the images in pseudocolor enhances the structural changes (Fig 2). This is achieved using a 256-level ''rainbow'' color table, as shown at the side of Figure 2. Figure 2 shows the SN_C of two control participants (C1 and C2) and two patients (P1 and P2). Note the presence of the substantia nigra pars reticulata in all cases reaching from the posterior SN_C across the crus cerebri toward the edge of the cerebral peduncle. The patient with early-stage Parkinson's disease (P1) shows lateral thinning and loss of signal in the SN_C. The lower section of the same patient shows islands of signal loss. Similar areas of signal loss were observed in the SN_C of all patients. The last row displays upper and lower sections for a patient with advanced-stage Parkinson's disease (P2). Note particularly the considerable signal loss and thinning of the SN_C in the medial segments of the upper section. The lower section shows severe thinning as well as two rims of relatively preserved signal.

Two observers evaluated the data. An experienced neurologist, blinded to the computation of the radiologic index, scored each patient by using the Unified Parkinson's Disease Rating Scale (2). The second observer, blinded to the identity of each participant, evaluated the radiologic indices for all participants. No interobserver reliability assessment was performed. Figure 3 shows that there is no overlap between patients and control participants and that the two groups are distinct ($P < .00005$, Student's t test). Figure 4 shows a high correlation

FIG 3. Radiologic indices are displayed for the six control participants and the six patients with Parkinson's disease. There is no overlap between the groups, which are distinct by Student's t test ($P < .00005$). The *error bars* represent one SD.

FIG 4. Unified Parkinson's Disease Rating Scale scores for the six patients ranging from 12 to 71 are plotted versus radiologic indices. A linear regression analysis was conducted, yielding a linear correlation coefficient of $r = 0.99$.

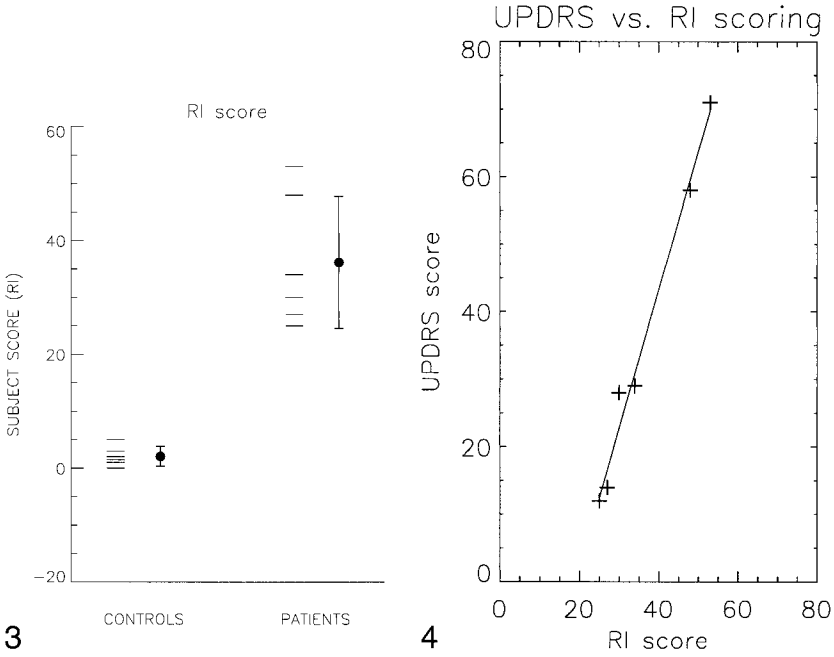

between radiologic index and Unified Parkinson's Disease Rating Scale score in the patient group ($r = 0.99$).

Discussion

The neuroimaging of the substantia nigra in Parkinson's disease by conventional MR imaging techniques has been a desirable but elusive goal. Potential benefits include the detection of presymptomatic disease as well as the staging of disease. Detection of presymptomatic disease, especially in the inherited disorder, would allow the early introduction of neuroprotective treatments in those determined to be at risk. Furthermore, the potential for staging the disease might allow assessment of neuroprotective interventions in both presymptomatic and symptomatic patients (19). Techniques of this kind may also serve to differentiate idiopathic Parkinson's disease from other forms of parkinsonism.

Visual inspection of the images confirms that the SN_C degenerates from lateral to medial and in an anterior-to-posterior direction. In addition, we note that in all six patients, there were zones of signal loss surrounded by rings of relative preservation in the lower section. These were not seen in any of the control participants. The significance of this particular pattern has yet to be ascertained and corroborated with neuropathologic findings. The sharp delineation of these structures, however, shows that the overall changes observed in the patient group were not the result of motion artifact. Artifacts of this kind tend to blur and degrade small structural changes.

The distinct separation of the patient from the control group in Figure 3 suggests the possibility of detecting presymptomatic disease. (Note that despite the relatively small number of participants in this study, the two groups were distinct at a high level of significance, $P < .00005$). Figure 4 suggests the possibility of staging disease progression with a radiologic index. The correlation between the Unified Parkinson's Disease Rating Scale score and the radiologic index is encouraging, although surprisingly high and probably somewhat fortuitous. As with any clinical scoring system, the Unified Parkinson's Disease Rating Scale values might fluctuate because of the performance of the patient, which can vary from day to day. An imaging technique capable of revealing the severity of the disease has several merits; among other things, it is independent of the physical condition of the patient and of the drugs used to control the symptoms.

Conclusion

A combination of two inversion-recovery sequences has been used to image in vivo the SN_C in healthy participants and in patients with Parkinson's disease. Lateral-to-medial neurodegeneration was confirmed visually in all six patients and allowed for definition of a simple radiologic index to score the severity of the disease. The radiologic index was found to be highly sensitive to even the earliest stages of disease and correlated strongly with the standardized clinical (Unified Parkinson's Disease Rating Scale) score in symptomatic patients. This suggests that MR imaging may not only have the potential for detecting presymptomatic disease but might also be used as a sensitive biological marker for disease progression in both presymptomatic and symptomatic patients. Such a marker could prove invaluable in the assessment of putative neuroprotective therapies. More work is

needed to refine the technique, in particular the use of faster pulse sequences and thinner sections.

Acknowledgments

This study was funded in part by the Myra Fox and Max Smedresman funds for research into Parkinson's disease.

References

1. Duvoisin RC. **Familial Parkinson's disease.** *Neurosci News* 1998;1:43–46
2. Barkats M, Bilang-Bleuel A, Buc-Caron MH, et al. **Adenovirus in the brain: recent advances in gene therapy for neurodegenerative diseases.** *Prog Neurobiol* 1998;55:333–341
3. Freese A. **Restorative gene therapy approaches to Parkinson's disease.** *Med Clin North Am* 1999;83:537–548
4. Fahn S, Elton ER. **Unified Parkinson's Disease Rating Scale.** In: Fahn S, Marsden CD, Calne D, Goldstein M, eds. *Recent Developments in Parkinson's Disease*. Florham Park, NJ: Macmillan Press;1987:293–304
5. Brooks DJ. **Motor disturbance and brain functional imaging in Parkinson's disease.** *Eur Neurol* 1997;38[suppl]:26–32
6. Shinotoh H, Calne DB. **The use of PET in Parkinson's disease.** *Brain Cogn* 1995;28:297–301
7. Sawle GV, Playford ED, Burn DJ, Cunningham VJ, Brooks DJ. **Separating Parkinson's disease from normality: discriminant function analysis of fluorodopa F 18 positron emission tomography data.** *Arch Neurol* 1994;51:237–243
8. Sawle GV. **The detection of preclinical Parkinson's disease: what is the role of positron emission tomography?** *Mov Disord* 1993;8:271–277
9. Seibyl JP, Marek K, Sheff K, et al. **Iodine-123-beta-CIT and iodine-123-FPCIT SPECT measurement of dopamine transporters in healthy subjects and Parkinson's patients.** *J Nucl Med* 1998;39:1500–1508
10. Seibyl JP, Marek KL, Quinlan D, et al. **Decreased SPECT beta-CIT striatal uptake correlates with symptom severity in Parkinson's disease.** *Ann Neurol* 1995;38:589–598
11. Vermeulen RJ, Wolters EC, Tissingh G, et al. **Evaluation of beta-CIT with SPECT in controls, early and late Parkinson's disease.** *Nucl Med Biol* 1995;22:985–991
12. Gorell JM, Ordidge RJ, Brown GG, Deniau JC, Buderer NM, Helpern JA. **Increased iron-related MRI contrast in the substantia nigra in Parkinson's disease.** *Neurology* 1995;45:1138–1143[published erratum appears in *Neurology*1995 ;45:1420]
13. Ordidge RJ, Gorell JM, Deniau JC, Knight RA, Helpern JA. **Assessment of relative brain iron concentrations using T2-weighted and T2*-weighted MRI at 3 tesla.** *Magn Reson Med* 1994;32:335–341
14. Antonini A, Leenders KL, Meier D, Oertel WH, Boesiger P, Anliker M. **T2 relaxation time in patients with Parkinson disease.** *Neurology* 1993;43:697–700
15. Moriwaka F, Tashiro K, Itoh K, Hamada T, Miyasaka K. **Magnetic resonance imaging in Parkinson's disease: the evaluation of the width of pars compacta on T2 weighted images [in Japanese].** *Rinsho Shinkeigaku* 1992;32:8–12
16. Mauricio JC, Coelho H, Sa J Martins A. **Importance of magnetic resonance in Parkinson disease: an analytic study of the pars compacta.** *Acta Med Port* 1990;3:85–88
17. Duguid JR, De La Paz R, DeGroot J. **Magnetic resonance imaging of the midbrain in Parkinson's disease.** *Ann Neurol* 1986;20:744–747
18. Fearnley JM, Lees AJ. **Aging and Parkinson's disease: substantia nigra regional selectivity.** *Brain* 1991;114:2283–2301
19. Brooks DJ. **The early diagnosis of Parkinson's disease.** *Ann Neurol* 1998;44[suppl 1]:S10–S18